

Cu₂SnS₃ FILMS SYNTHESIS DURING ANNEALING OF 2Cu:1Sn METALL ALLOY LAYERS IN SULFUR VAPOR

A.V. BUDANOV^a, YU. N. VLASOV^{a,*}, G. I. KOTOV^a, E.V. RUDNEV^b,
A. A. VINOKUROV^c

^a*Voronezh State University of Engineering Technologies, 19 Revolution Av.,
Voronezh, Russia*

^b*Voronezh State University, 1 Universitetskaya pl., Voronezh, Russia*

^c*Voronezh State Technical University, 14 Moskovsky Av., Voronezh, Russia*

Cu₂SnS₃ films are formed on glass substrates by annealing in sulfur vapor of a metal layer of composition Cu:Sn = 2:1 in a vacuum graphite chamber of the quasi-closed volume at a synthesis temperature of 400 ° C. By X-ray spectral microanalysis, it was established that the stoichiometry of the sulfide film corresponds to the Cu₂SnS₃ compound. The X-ray diffraction method has shown that the forming Cu₂SnS₃ film has a cubic crystal sphalerite-type lattice of the F-43m symmetry group with a lattice parameter of 5.38 Å. The activation energy of optical direct-gap transitions of a film determined by IR spectroscopy is 0.95 eV and corresponds to the cubic modification of Cu₂SnS₃. An estimation of the absorption coefficient of light in the visible region of the spectrum gives a value of the order of 2·10⁵ cm⁻¹. The calculation of the minimum thickness of the Cu₂SnS₃ layer, necessary for the absorption of most of the photons in the visible spectrum gives a value on the order of 200 nm. Such thickness is comparable to the size of the crystallites of the forming film, and this makes it possible to use the proposed technology to form active layers of Cu₂SnS₃-based solar cells.

PACS numbers: 81.20.-n, 61.10.Nz, 84.60.Jt

Received March 31, 2019; Accepted June 7, 2019)

Keywords: Ternary sulfides, Quasi-closed volume, Solar cells

1. Introduction

In recent years a direct-gap Cu₂SnS₃ (CTS) p-type ternary compound has been proposed as a photoactive layer for thin-film solar cells (SCs). It has a high absorption coefficient of about 10⁴ ÷ 10⁵ cm⁻¹ in the visible region of the solar spectrum and an optimal band gap of 1.0–1.5 eV [1]. Interest in this compound is associated with the absence of toxic and expensive rare-earth elements in its composition, such as Ga and In [2].

The instability of the five-component chalcogenide Cu₂ZnSn(S,Se)₄ does not allow the creation of thin-film SCs based on it with power efficiency of more than 12% [3]. The five-component chalcogenide is difficult to obtain, has a very narrow region of existence. Phase inclusions of binary and ternary compounds, such as SnS, ZnS and CTS, are observed in the volume of the formed Cu₂ZnSn(S,Se)₄ films [4]. At the same time, chemically more stable CTS films with a thickness of about 1 micron can be formed by a significantly less expensive two-stage process, which involves the deposition of a metal precursor (Cu-Sn) on a substrate followed by annealing in a sulfur-containing inert atmosphere Ar [5].

In the literature [1–8], methods for the synthesis of CTS films during the heterophase sulfurization reaction of a multilayer Cu – Sn precursor deposited on a substrate by magnetron sputtering of copper and tin metal layers were described. From the point of view of the phase composition homogeneity of the film with minimal inclusion of secondary phases, the optimum atmosphere pressure (resulting from the partial pressures of inert gas and sulfur vapor) in the sulfurization process ranges from 1 to 100 Pa [6]. In the case of lower pressure, the formation of

* Corresponding author: youramail@mail.ru

double tin chalcogenides, such as Sn_2S_3 and SnS , along with Cu_2SnS_3 , is possible [5,6]. In this case, the effect of displacement of the $\text{Cu}:\text{Sn} = 2:1$ stoichiometric ratio toward copper depletion and tin enrichment due to evaporation of volatile SnS tin monosulfide from the surface of the forming film becomes significant [7,8]. An excessively high pressure may contribute to the formation of Cu_4SnS_4 and $\gamma\text{-Cu}_2\text{S}$ compounds [6]. The optimum temperatures for the formation of a Cu_2SnS_3 film with a homogeneous phase composition during the sulfurization of a metal precursor in sulfur vapors, according to a number of papers [5, 6, 7], are in the range from 400 to 570 °C.

The purpose of this work is to obtain Cu_2SnS_3 sulfide layers on a glass substrate according to a two-step technique: deposition of a metal precursor layer ($\text{Cu}:\text{Sn} = 2:1$ alloy) on the substrate followed by annealing in sulfur vapor in a graphite chamber of the quasi-closed volume type. The study of the structure, morphology and optical properties (band gap, absorption coefficient) of CTS layers was carried out. The calculation of the optimal thickness of the CTS photoactive layer for use in the SC was carried out.

2. Experimental

To create an alloy of atomic composition $\text{Cu}:\text{Sn} = 2:1$ of a thin-film precursor weighed metals were mixed, placed in a quartz vacuum ampoule, and heated to a temperature above the melting point of copper, at 1150 °C for 1 hour. The composition of the samples was monitored by X-ray microanalysis using a JSM 840 instrument with wavelength dispersion. The glass substrates were washed in a solution of $\text{K}_2\text{Cr}_2\text{O}_7$ in concentrated sulfuric acid, followed by washing in distilled water. Films from 0.14 to 0.40 μm thick were deposited by thermal evaporation from an alloy onto a glass substrate, which was monitored using an MII-4 microinterferometer and a scanning electron microscope. The composition of the films was determined by X-ray microanalysis using a JSM-6380LV JEOL electron microscope with the INCA 250 microanalysis system. The detected ratio of $\text{Cu}:\text{Sn} = 1.9 \div 2.0$ in the metal film deposited by thermal spraying is due to the proximity of the partial pressures of the Cu and Sn vapors at the evaporation temperature [9]. Then, heat treatment of metal films in a vacuum chamber in a quasi-closed graphite volume at a substrate temperature of 400 °C and a partial pressure of sulfur vapor about 1 Pa was carried out. The duration of the treatment process ranged from 10 minutes to 35 minutes, depending on the thickness of the metal film. X-ray phase analysis of sulfide films was carried out on a DRON-5 with an X-ray CoK_α source. The optical properties of the synthesized CTS films were studied on a Bruker MPA two-beam IR spectrophotometer and in the visible light range using a SPEX SSP-715-M dual-beam spectrophotometer. The morphology of the CTS surface was studied in a scanning electron microscope and atomic force microscopy using a FemtoScan-1. The surface resistance of the films was estimated using the four-probe method.

3. Results and discussion

Fig. 1 shows the diffraction patterns of CTS films. They contain peaks corresponding to reflections from the (111), (220) and (311) planes. This is characteristic of the cubic Cu_2SnS_3 phase of the F-43m symmetry group (PDF 01-089-2877). The two remaining intense peaks at angles of $2\Theta = 30.5^\circ$ and 37.3° can correspond to tin monosulfide SnS (PDF 00-039-0354). The peak with $2\Theta = 37.3^\circ$ can also correspond to the $\text{Cu}_{1.8}\text{S}$ compound of the F-m-3m symmetry group (PDF 00-056-1256). It is known that Cu_2SnS_3 compound crystallizes in cubic, tetragonal and monoclinic modifications depending on the degree of ordering of atoms in the cation sublattice [7,10]. The atomic structures of the crystal lattices of the cubic, tetragonal, and monoclinic modifications are similar, and this makes it difficult to identify them according to the results of X-ray diffraction studies [7]. The average value of the crystal lattice spacing for synthesized CTS films, calculated from the three experimental values of the interplanar distances d_{111} , d_{220} and d_{311} , is equal to 5.38 Å. The known lattice parameter of the Cu_2SnS_3 cubic phase is 5.43 Å (PDF 01-089-2877).

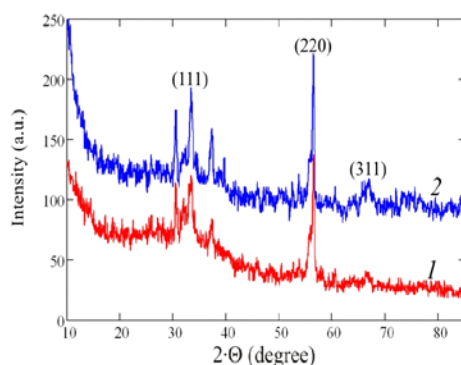


Fig. 1. Diffractograms of CTS films formed by annealing in sulfur vapor at a substrate temperature of 400 °C (1 - the thickness of the initial metallization layer is 0.14 μm , the processing time is 20 minutes; 2 - the thickness of the initial metallization layer is 0.40 μm , the processing time is 35 minutes).

The elemental composition of CTS films, determined by X-ray microanalysis, corresponds to the stoichiometric ratio of elements for Cu_2SnS_3 (in atomic %): Cu - 32.0; Sn — 14.8; S - 53.2. In this case, copper enrichment $\text{Cu}:\text{Sn} = 2.1 \div 2.2$ in the process of thermal annealing in sulfur vapor can occur due to evaporation from the surface of more volatile tin sulfides [7, 8].

AFM images of the surface of CTS films are shown in Figure 2. Most of the surface of the film has the form shown in Fig. 2, a. With a film thickness of 250 nm and lateral dimensions of CTS 200 \div 300 nm crystallites, the average size of the heterogeneity in height is ± 50 nm, while the roughness of the initial glass substrate does not exceed ± 10 nm.

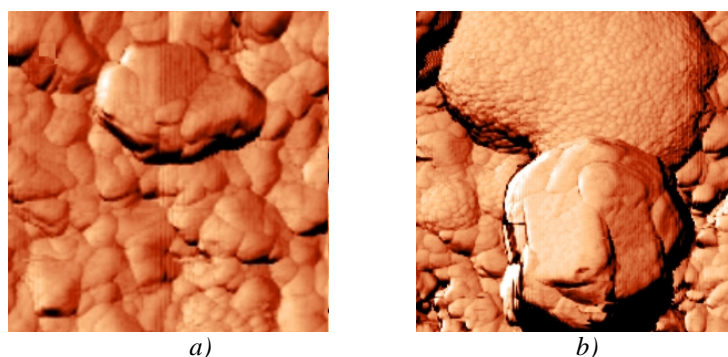


Fig. 2. AFM image of $2 \times 2 \mu\text{m}^2$ of the surface of the CTS film formed by annealing in sulfur vapor at a substrate temperature of 400 °C for 20 minutes (a is the topology of the majority of the surface, b is the surface with secondary phases deposited).

On the surface, crystallites of a hexagonal shape of lateral size 1 μm and a height of 0.5 μm with a density of 10^4mm^{-2} are observed (Figure 2, b). Such crystallites may correspond to the secondary phase of copper sulfide $\text{Cu}_{1.8}\text{S}$, while an array of much smaller crystallites with a size of 20 nm may correspond to the secondary phase of tin sulfide SnS. This assumption is based on our earlier study of the morphology of the surfaces of copper sulphide and tin sulphide films synthesized by sulfurization of pure copper and tin metals layers under conditions similar to those of the CTS film synthesis [11].

Figure 3 shows the transmission spectra of CTS films with a thickness of 250 nm in the visible wavelength range (Figure 3, a) and in the IR range (Fig. 3, b). The spectrum in Figure 3a is used to determine the activation energy of direct-gap transitions as 1.53 eV (in the wavelength range $\lambda = 520 \div 720$ nm with Pearson's linear correlation coefficient $k = 0.929$) and 1.04 eV ($\lambda = 780 \div 960$ nm with $k = 0.993$). The spectrum in Fig. 3, b shows the activation energies of

direct-gap transitions as 0.95 eV ($\lambda = 880 \div 1050$ nm with $k = 0.996$) and 0.52 eV ($\lambda = 1530 \div 2000$ nm with $k = 0.999$).

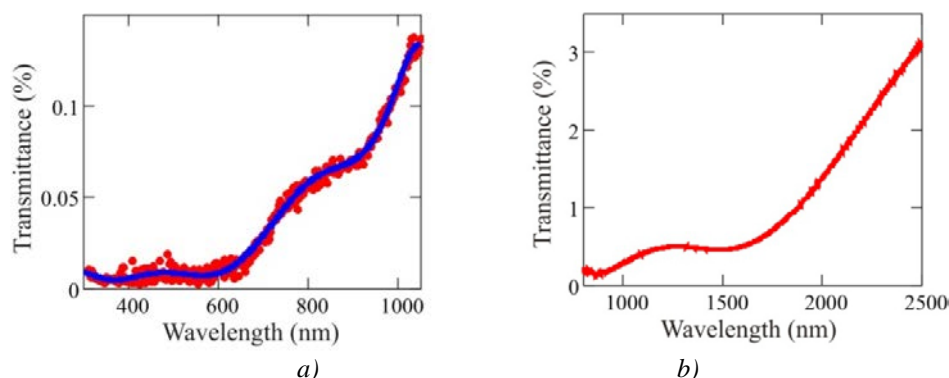


Fig. 3. Optical transmission spectra of a CTS film formed by annealing in sulfur vapor at a substrate temperature of 400 °C for 20 minutes (a - in the visible range of light wavelengths, b - in the IR range).

The values of 0.95 eV and 1.04 eV are close and correspond to the band gap of the Cu_2SnS_3 compound [7, 12]. According to some authors [5], the presence of transitions with an activation energy of 1.06 eV is due to the presence of the secondary phase Cu_3SnS_4 in the CTS film. From the point of view of other authors [13], the appearance of direct-gap transitions of two energies of 0.94 eV and 1.04 eV in the spectrum of the external quantum efficiency of the finished SC based on the CTS film with a homogeneous phase composition is determined by the band structure of this material. The latter opinion is confirmed by theoretical modeling of Cu_2SnS_3 band structure [14].

The value of 0.52 eV is probably due to transitions in a double compound of the Cu_{2-x}S , whose band gap ranges from 0.4 to 0.6 eV, as follows from the theoretical studies [15]. The activation energy of 1.53 eV corresponds to the width of the SnS band gap [16]. The values of the absorption coefficient for the CTS film determined in this work range from $1.5 \cdot 10^5 \text{ cm}^{-1}$ to $3 \cdot 10^5 \text{ cm}^{-1}$ in the wavelength range of light from 2500 nm to 400 nm, respectively (see Fig. 3).

The resistivity of the films is in the range from 0.1 to 1 $\Omega \cdot \text{cm}$. High conductivity of CTS films can be associated with the presence of the secondary phases such as narrow-gap copper sulfides of the Cu_{2-x}S type, which are also observed in the transmission spectra of films in the visible part of the spectrum.

4. Calculations

The optimal thickness of the CTS photosensitive layers was calculated for the n-ZnS/p-CTS heterojunction as the most promising in our opinion for producing an SC due to the coincidence of the crystal structure and matching the lattice parameter of these materials – the ZnS lattice parameter is 5.41 Å [10]. This problem was solved by simulating the current-voltage characteristics of the SC. To estimate the proportion of photons that penetrate a certain depth of the photoactive material, we used the spectral dependence of the absorption coefficient on the wavelength $\alpha(\lambda)$ and the spectral distribution $S(\lambda)$ of the intensity of sunlight (AM 1.5). The dependence $\alpha(\lambda)$ is determined by approximating the solid blue line $T(\lambda)$ in Figure 3, a. The number of photogenerated electron-hole pairs was determined by the number of absorbed photons at a certain depth of the absorber. The scattering of minority carriers in n-ZnS and p-CTS was determined through diffusion lengths. The value of L_p for n-ZnS was taken from the literature data of [17], and L_n for p-CTS was determined by the mobility and lifetime of charge carriers.

The charge carriers diffusion coefficient D in dependence of their mobility μ was calculated by the formula

$$D = \frac{k \cdot T \cdot \mu}{q_e}, \quad (1)$$

where k is the Boltzmann constant, $T = 300$ K is the temperature, and q_e is the elementary charge.

The diffusion length L of charge carriers, which are minor for a given material, was determined depending on their lifetime τ by the formula

$$L = \sqrt{D \cdot \tau}. \quad (2)$$

The function of the generation rate of electron-hole pairs in the emitter regions (upper n-ZnS layer) and base (lower p-CTS layer) of the heterojunction on the light penetration depth x was set by integration in accordance with formulas (3) and (4):

$$G_{\text{ZnS}}(x) = q_e \int_{\lambda_{\min}}^{\lambda_{\max}} S(\lambda) (1 - e^{-\alpha_{\text{ZnS}}(\lambda) \cdot x}) \cdot d\lambda; \quad (3)$$

$$G_{\text{CTS}}(x) = q_e \int_{\lambda_{\min}}^{\lambda_{\max}} S(\lambda) e^{-\alpha_{\text{ZnS}}(\lambda) \cdot d_{\text{ZnS}}} (1 - e^{-\alpha_{\text{CTS}}(\lambda) \cdot x}) \cdot d\lambda, \quad (4)$$

where $\lambda_{\min} = 300$ nm, $\lambda_{\max} = 1100$ nm are the limits of integration over the wavelengths of the incident light. The thickness of the emitter layer is denoted as d_{ZnS} .

The emitter current and base current were calculated using formulas (5) and (6), respectively:

$$I_{\text{ZnS}} = \int_0^{d_{\text{ZnS}}} \left(\frac{dG_{\text{ZnS}}(x)}{dx} \right) e^{-\frac{d_{\text{ZnS}} - x}{L_{\text{ZnS}}}} \cdot dx, \quad (5)$$

$$I_{\text{CTS}} = \int_0^{d_{\text{CTS}}} \left(\frac{dG_{\text{CTS}}(x)}{dx} \right) e^{-\frac{x}{L_{\text{CTS}}}} \cdot dx, \quad (6)$$

where d_{CTS} is the thickness of the base layer.

The short circuit current I_{sc} was defined as the sum of the base and emitter currents:

$$I_{\text{sc}} = I_{\text{ZnS}} + I_{\text{CTS}}. \quad (7)$$

It has been established that for the values of the absorption coefficient we determined, the optimal thickness of the CTS layer does not exceed 300 nm (Figure 4). It is seen that with an increase in film thickness of more than 300 nm, the short circuit current density does not increase, since almost all light is absorbed by a CTS film of such thickness.

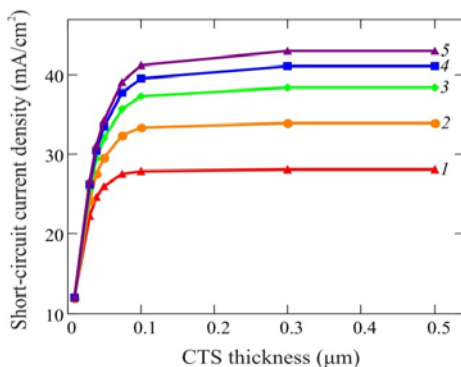


Fig. 4. Dependence of the short circuit current density on the thickness of the photoactive p-CTS layer for the n-ZnS/p-CTS heterojunction, at different values of the diffusion length L of minority charge carriers in p-CTS. (1 - $L_n = 50$ nm, 2 - $L_n = 100$ nm, 3 - $L_n = 200$ nm, 4 - $L_n = 400$ nm, 5 - $L_n = 1000$ nm).

When the diffusion length of minority charge carriers L_n is 200 nm (comparable to the crystallite size, Fig. 2), the short-circuit current is saturated. Therefore, in accordance with formulas (1) and (2), the maximum value of the short circuit current can be achieved already with acceptable values of electron mobility in the p-CTS layer from 1 to 150 cm²V⁻¹s⁻¹ and the lifetime from 10 to 0.1 ns, respectively. Since such values of electron mobility and lifetime are achievable in vacuum thin-film technology, CTS films synthesized according to the method described above can be used in SC structures.

4. Conclusions

This paper shows the possibility of using as a precursor a two-component metal layer deposited on a substrate by thermal spraying of an alloy of composition 2Cu:1Sn. In the process of annealing in sulfur vapor, the three-component compound Cu₂SnS₃ crystallizes in the cubic lattice of the F-43m symmetry group. The lattice parameter is equal to 5.38 Å. X-ray microanalysis has shown that the elemental composition of the films corresponds to the stoichiometry of the Cu₂SnS₃ compounds. The activation energies of direct-gap transitions of the synthesized Cu₂SnS₃ compound are determined by us as 0.95 eV, which corresponds to its cubic modification [13,14, 18].

The thickness of the CTS photoactive layer for use in the SC was calculated, taking into account the experimentally established spectral dependence of the absorption coefficient of the synthesized films. It is shown that a sufficient thickness of the CTS layer is comparable with the crystallite size. At the same time, X-ray diffraction and transmission spectroscopy revealed the inclusion of secondary phases of sulfides like SnS and Cu_{2-x}S. The presence of copper sulfides in the CTS film can lead to an increase in conductivity and light absorption coefficient. CTS layers that are more homogeneous in phase composition can be formed by compensating for the effect of tin depletion as a result of high-temperature annealing of CTS during synthesis of a 1.9Cu:1Sn precursor and an increase in sulfur vapor pressure [6,7]. An increase in the treatment temperature in sulfur vapor can lead to the enlargement of crystallites, which is useful for reducing the influence of the crystallite boundaries of the photoactive layer on the final characteristics of the SC.

Acknowledgments

This work is financially supported by Russian Foundation for Basic Research, Russian Federation (RFBR Grant 18-32-00971).

References

- [1] M. Hegedus, M. Balaz, M. Tesinsky et al., *Journal of Alloys and Compounds* **768**(5), 1006 (2018).
- [2] H. Wesley, *Renewable and Sustainable Energy Reviews* **77**, 590 (2017).
- [3] W. Wang, M. T. Winkler, O. Gunawan et al., *Adv. Energy Mater* **4**, 1 (2014).
- [4] S. Das, K. C. Mandal, R. N. Bhattacharya, *Semiconductor Materials for Solar Photovoltaic Cells*, 25 (2015).
- [5] Mohan Reddy Pallavolu et al., *Applied Surface Science* **462**, 641 (2018).
- [6] Pin-Wen Guan, Shun-Li Shang, Gret Lindwall, Tim Anderson, Zi-Kui Liu, *Solar Energy* **155**, 745 (2017).
- [7] A. C. Lokhande et al., *Solar Energy Materials and Solar Cells* **153**, 84 (2016).
- [8] Weihuang Wang et al. *Journal of Alloys and Compounds* **742**, 860 (2018).
- [9] O. Y. Subbotina, N. V. Kishkoparov, I. V. Frishberg, *High Temperature* **37**, 198 (1999).
- [10] Y. Ren, Y. Doktoravhandling, Uppsala, 2017, 85 p.
- [11] A. V. Budanov et al. *Condensed matter and interphases* **18**, 481 (2016).

- [12] Mingrui He et al. *Journal of Alloys and Compounds* **701**, 901 (2017).
- [13] K. Suzuki et al. *Applied Surface Science* **414**, 140 (2017).
- [14] A. Crovetto et al., *Sol. Energy Mater. Sol. Cells* **154**, 121 (2016).
- [15] P. Lukashev, W. R. L. Lambrecht, T. Kotani, M. Schilfgaard, *Phys. Rev. B* **76**, 195202 (2007).
- [16] Martin Parenteau and Cosmo Carlone *Phys. Rev. B* **41**, 5227 (1990).
- [17] Jiaxiong Xu, Yuanzheng Yang. *Energy Conversion and Management* **78**, 260 (2014).
- [18] Ejarder Sabbir Hossain et al. *Current Applied Physics* **18**, 79 (2018).